doi:10.1006/jmbi.2001.4706 available online at http://www.idealibrary.com on IDEAL® *J. Mol. Biol.* (2001) **309**, 641–655

JMB

# Subcellular Localization and Oligomerization of the *Arabidopsis thaliana* Somatic Embryogenesis Receptor Kinase 1 Protein

**Khalid Shah, Theodorus W. J. Gadella Jr, Harrie van Erp, Valérie Hecht and Sacco C. de Vries***

*Laboratory of Molecular Biology, Department of Plant Sciences, Wageningen University and Research Centre, Wageningen, The Netherlands*

**Corresponding author*

The *Arabidopsis thaliana somatic embryogenesis receptor kinase* 1 (*AtSERK1*) gene is expressed in developing ovules and early embryos. *AtSERK1* is also transiently expressed during somatic embryogenesis. The predicted AtSERK1 protein contains an extracellular domain with a leucine zipper motif followed by five leucine-rich repeats, a proline-rich region, a single transmembrane region and an intracellular kinase domain. The *AtSERK1* cDNA was fused to two different variants of green fluorescent protein (GFP), a yellow-emitting GFP (YFP) and a cyan-emitting GFP (CFP), and transiently expressed in both plant protoplasts and insect cells. Using confocal laser scanning microscopy it was determined that the AtSERK1-YFP fusion protein is targeted to plasma membranes in both plant and animal cells. The extracellular leucine-rich repeats, and in particular the N-linked oligosaccharides that are present on them appear to be essential for correct localization of the AtSERK1-YFP protein. The potential for dimerization of the AtSERK1 protein was investigated by measuring the YFP/CFP fluorescence emission ratio using fluorescence spectral imaging microscopy. This ratio will increase due to fluorescence resonance energy transfer if the AtSERK1-CFP and AtSERK1-YFP fusion proteins interact. In 15% of the cells the YFP/CFP emission ratio for plasma membrane localized AtSERK1 proteins was enhanced. Yeast-protein interaction experiments confirmed the possibility for AtSERK1 homodimerization. Elimination of the extracellular leucine zipper domain reduced the YFP/CFP emission ratio to control levels indicating that without the leucine zipper domain AtSERK1 is monomeric.



*Keywords:* AtSERK1; green fluorescent protein; glycosylation; oligomerization; fluorescence resonance energy transfer

## Introduction

Receptor kinases have been shown to play a key role in developmental processes such as cell proliferation, migration and differentiation. Receptor kinase-mediated signal transduction pathways are highly conserved in both vertebrates and invertebrates.[1,2] In plants, similar receptors, designated as receptor-like kinases (RLKs) also appear to play a crucial role in development.[3]

The classical model for receptor kinase-activation involves ligand binding-induced dimerization of the receptor, resulting in autophosphorylation of both partners in the dimer, mainly on specific tyrosine, serine or threonine residues. The best known examples of this mode of action are the transforming growth factor (TGF-β) receptor and the epider-

Abbreviations used: *AtSERK1*, *Arabidopsis thaliana* somatic embryogenesis receptor kinase 1; LZ, leucine zipper; LRR, leucine-rich repeat; GFP, green fluorescent protein; YFP, yellow-emitting GFP; CFP, cyan-emitting GFP; CLSM, confocal laser scanning microscopy; FSPIM, fluorescence spectral imaging microscopy; FRET, fluorescence resonance energy transfer; RLK, receptor-like kinase; TGF-β, transforming growth factor β; EGF, epidermal growth factor; SRK, S-locus receptor kinase; *CLV*, *CLAVATA*; BRI1, Brassinosteroid insensitive 1; *SERK*, somatic embryogenesis receptor kinase gene; IL1, interleukin 1; FCS, fluoresence correlation spectroscopy; AD, activation domain, BD, binding domain; 2,4-D, 2,4-dichlorophenaxy acetic acid; EGFR, epidermal growth factor receptor; PDGFR, platelet derived growth factor receptor.

E-mail address of the corresponding author: Sacco.deVries@mac.mb.wau.nl

0022-2836/01/030641–15 $35.00/0

mal growth factor (EGF) receptor.[4] Ligand-induced dimerization of cell surface receptors can bring into proximity downstream proteins associated with these receptors followed by transphosphorylation of such target proteins. Animal receptor kinases can dimerize either by ligand-dependent non-covalent dimerization[5] or by ligand-independent covalent dimerization.[6] Dimerization can involve two identical receptors (homodimerization); different members of the same receptor family or a receptor and an accessory protein (heterodimerization).[7] Receptor activation through heterodimerization is the most common,[4] but certain receptors such as those for growth hormones employ homodimerization.

The evidence for monomer to dimer transition as a mechanism for receptor activation derives from experiments demonstrating that ligand binding leads to receptor dimerization.[4] Second, artificially induced dimerization or naturally occurring mutations leading to dimerization both mimic signaling in the absence of the physiological ligand.[8,9] Finally, oligomerization of intracellular regions of receptors using cell permeable synthetic ligands can lead to dimerization.[10] However, one of the most extensively studied eukaryotic receptors, the insulin receptor, exists as an inactive ($\alpha\beta$) dimer maintained by intersubunit disulfide cross bridges.[11]

The mechanisms by which plant receptors transduce signals across the cell surface are largely unknown but plant receptors may also dimerize.[12] Studies on the action of the S-locus receptor kinase (SRK), involved in the self-incompatibility response in *Brassica*, have shown that recombinant SRK autophosphorylates constitutively and exists as dimers in nonpollinated stigmas.[13] The *CLAVATA* (*CLV*) genes control cell proliferation in the *Arabidopsis* shoot and inflorescence meristems. It has been shown that the CLV3 peptide acts as a ligand in the CLV1/CLV2 receptor complex.[14–16] Recent chimeric studies on RLKs, using the extracellular domain of brassinosteroid insensitive1 (BRI1) protein, involved in the perception of brassinosteroids and the intracellular domain of the Xa21 protein, involved in pathogen resistance from rice have revealed that the use of chimeric receptors may also highly useful in plants.[17]

Transmembrane receptor proteins, like other cell surface proteins undergo post-translational modifications such as disulfide bonding, glycosylation, palmitoylation and proteolytic cleavage. Many of these modifications play decisive roles in protein maturation and/or intracellular trafficking.[18] In mammalian cells, the correct folding and oligomerization of complex, multi-domain secretory proteins is controlled by *N*-glycosylation.[19] For example, the human insulin receptor has several glycosylation sites close to the N terminus of the receptor. Mutational analysis of these sites showed that glycosylation was essential for correct processing and targeting of the protein to the cell surface.[20] In plant RLKs such studies have not been conducted, but the predicted protein sequence of plant RLKs shows that similar domains close to the N terminus contain N-linked glycosylation sites.

Somatic embryogenesis is the process whereby somatic cells can develop into plants *via* characteristic morphological stages. In cultured *Daucus carota* suspension cells, the *SERK* (somatic embryogenesis receptor kinase) gene, a leucine-rich repeat (LRR)RLK, was found to be a marker for single suspension cells capable of forming embryos.[21] During somatic and zygotic embryogenesis *SERK* expression continues up to the early globular stage and is absent in later stages of embryo development. The most closely related *Arabidopsis thaliana SERK1* gene is expressed in developing ovules, early embryos and in vascular tissues of seedlings (V. Hecht *et al*., unpublished results). The predicted AtSERK1 protein contains an N-terminal leucine zipper (LZ), five LRRs and a proline-rich region in its predicted extracellular domain. This is followed by a single transmembrane domain that is attached to an intracellular kinase domain with all 11 conserved subdomains as found in serine/threonine kinases (V. Hecht *et al*., unpublished results).

Based on the jelly fish green fluorescent protein (GFP) and confocal microscopy, spatiotemporal dynamics of GFP-fusion proteins in intact cells can be investigated.[22–24] We have used AtSERK1-GFP fusion proteins to determine the subcellular localization of this receptor. In addition, dimerization of the chimeric proteins was investigated making use of fluorescence resonance energy transfer (FRET) by employing spectroscopic variants of GFP. FRET is a quantum-mechanical process by which the excitation energy is transferred from a donor fluorochrome to an appropriate acceptor fluorochrome. FRET only occurs when: (i) the donor fluorophore emission spectrum overlaps with the absorption spectrum of the acceptor, (ii) the transition dipole moments of the donor and the acceptor are not perpendicularly oriented, and (iii) the distance between the donor and the acceptor is less than 1.5× the Förster radius ($R_0$) for energy transfer.[25,26] Different engineered spectral variants of GFP, exhibiting yellow or cyan fluorescence, (YFP and CFP, respectively) provide an opportunity to label the same protein with two different fluorophores in the same living cell.[27] More importantly, the emission and the excitation spectrum of these two variants of GFP are suitable for FRET. This allows to probe proximity of proteins in intact living cells.[28] The $R_0$ for CFP/YFP FRET is 5.5 nm implying that FRET between CFP and YFP will only be detected when the proximity of the fluorophores is less than 10 nm. FRET is manifested in different ways: a decrease in donor fluorescence quantum yield, a decreased donor fluorescence lifetime, an increased stability of the donor towards chemical photobleaching[29] and an increased sensitized acceptor fluorescence emission, if the acceptor is a fluorophore.[30,31] FRET microscopy[28] has been successfully employed to investigate the assembly of

the T-cell antigen receptor complex,[32,33] the interleukin-1 (IL-1) receptor complex after IL-1 binding[34] and to study EGF receptor oligomerization.[35,36]

The results presented here show that the AtSERK1 protein is localized in the plasma membrane, mainly in the form of monomers. Only a small percentage of the AtSERK1 protein may exist as oligomers (e.g. homodimers), suggesting that the AtSERK1 protein belongs to a class of receptors that can undergo ligand-dependent non-covalent homodimerization. Employing truncated AtSERK1 proteins, it was found that the LRR domain is involved in correct targeting of the receptor while the LZ domain is involved in receptor dimerization.

## Results

### AtSERK1-YFP/CFP fusion proteins

Here, several AtSERK1-YFP/CFP constructs were used. These constructs are shown in detail in Figure 1. In order to determine the localization of the AtSERK1 protein, several AtSERK1-YFP constructs (Figure 1(b), (d), (f) and (h)) were transfected into cowpea mesophyll protoplasts. After incubation for 12 hours, soluble and pellet fractions were isolated, separated by denaturing SDS-PAGE and immunoblotted using an antiserum raised against GFP (Figure 2). The results show that AtSERK1-YFP wild-type, AtSERK1ΔLZ-YFP and AtSERK1ΔLRR-YFP proteins are all found exclusively in the pellet fraction. Upon deletion of the entire extracellular domain and the transmembrane domain (Figure 1(d)), about 40% of the protein becomes soluble, while the remainder is present in the pellet fraction (Figure 2). We conclude that the AtSERK1-YFP fusion proteins are correctly expressed and that the majority are present in the insoluble pellet fractions that may represent the membrane fraction.

### Localization and targeting of AtSERK1 protein

To determine whether AtSERK1-YFP fusion proteins were localized in the plasma membrane, viable transfected protoplasts were analyzed by confocal laser scanning microscopy (CSLM) 12 hours after transfection. Protoplasts transfected with an AtSERK1-YFP construct (Figure 1(b)) clearly showed fluorescence at the surface of the protoplasts (Figure 3(a)). Endomembranes were labeled to a lesser extent, possibly reflecting proteins in transit. In contrast, cytoplasmic expression was observed when the pMON999-YFP vector alone (Figure 3(c)) or the AtSERK1$^{kin}$-YFP construct (Figure 1(d)) was transfected into protoplasts (Figure 3(b)). The EGFR$^{ex}$-AtSERK1$^{kin}$-YFP construct (Figure 1(n)), was also expressed in protoplasts and the chimeric protein showed the same predominant surface localization (Figure 3(d)) as that of the AtSERK1-YFP protein. The EGF receptor is a true plasma membrane receptor with cysteine-rich repeats in the extracellular domain. The correspondence in the location of fluorescence between the AtSERK1 and the chimeric EGFR-AtSERK1 receptor strongly suggests that AtSERK1 is a plasma membrane-localized protein.

To confirm the AtSERK1 protein localization in the plasma membrane, the AtSERK1$^{ins}$-YFP-CFP fusion construct (Figure 1(y)) was expressed in *Spodoptera frugiperda* (Sf21) insect cells in order to perform fluorescence correlation spectroscopy (FCS). A line-scan along the optical axis (*z*-axis) was made to determine the distribution of fluorescent proteins in the cell. Detection of fluorescent fusion proteins by the sensitive, single molecule detection, FCS technique is more convenient in insect cells than in plant protoplasts because of the absence of background chlorophyll autofluorescence. The AtSERK1$^{ins}$-CFP-YFP expressing cells showed the same low intensity of 20 kHz (photoelectrons emitted per second) in the nuclear region as in the non-infected cells. There was a three- to fourfold (161 kHz) increase in the fluorescence intensity in the plasma membrane region of AtSERK1$^{ins}$-CFP-YFP expressing cells (Figure 3(f)) as compared to highest fluorescence intensity of around 40 kHz in the plasma membrane of the non-infected Sf21 cells (Figure 3(e)). This finding indicates that the AtSERK1$^{ins}$-CFP-YFP proteins are also correctly localized in the plasma membrane in insect cells. In cells expressing the fusion proteins to a very high level, also endomembranes were labelled, possibly reflecting proteins in transit or undergoing endocytosis (data not shown).

To determine whether the extracellular LZ domain and the different LRRs of the AtSERK1 protein have a role in targeting of the AtSERK1 receptor we transfected protoplasts with a series of constructs in which the LZ domain or one or several LRRs were removed (see Figure 1(b), (f), (h), (j)-(m) for an overview of the constructs used). Protoplasts expressing the AtSERK1ΔLZ-YFP protein showed the same surface fluorescence as shown by protoplasts expressing AtSERK1-YFP (Figure 4(a), compare with Figure 3(a)). No effect of the removal of the first LRR was evident after transfecting AtSERK1ΔLRR$^{1}$-YFP into protoplasts (Figure 4(b)). There was some decrease in surface fluorescence when AtSERK1ΔLRR$^{1,2}$-YFP (Figure 4(c)) or AtSERK1ΔLRR$^{1,2,3}$-YFP (Figure 4(d)) were transfected into protoplasts. In addition to the plasma membrane, the truncated AtSERK1 proteins were also seen in subcellular organelles. There was a considerable decrease in surface fluorescence when AtSERK1ΔLRR$^{1,2,3,4}$-YFP was transfected into protoplasts (Figure 4(e)). Most of the AtSERK1 protein was seen to be concentrated in subcellular organelles which might represent clogging in ER or Golgi-derived vesicles or sequestering of the AtSERK1 protein in the lysosomal compartments of the protoplasts (Figure 4(e)). Upon transfection of AtSERK1ΔLRR-YFP into protoplasts, almost no

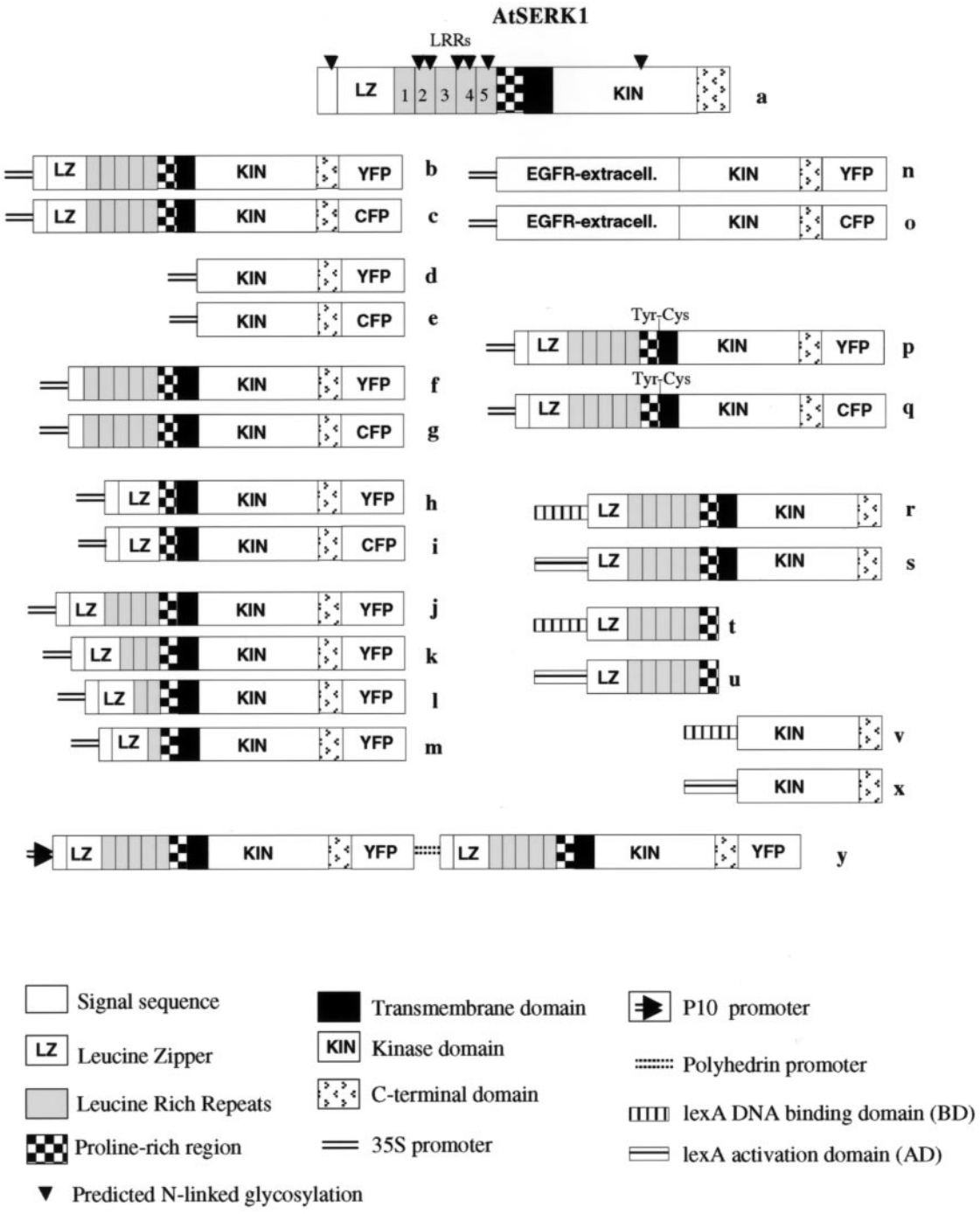


**Figure 1** (*legend shown opposite*)

surface fluorescence was observed (Figure 4(f)). Most of the fusion protein was seen internally as in Figure 4(e). We conclude that the LZ domain of AtSERK1 is not involved in protein targeting but that at least four LRRs of AtSERK1 contain specific information for correct targeting of the AtSERK1 protein.

The AtSERK1 protein contains seven predicted *N*-glycosylation sites, five of which are present in the LRRs of the extracellular domain (Figure 1(a)). To determine whether these sites are used in the proper targeting of the AtSERK1 protein, we treated the protoplasts with 20 μg $ml^{-1}$ tunicamycin three hours after transfection with AtSERK1-YFP. Tunicamycin prevents the addition of *N*-acetylglucosamine to dolichol phosphate, the first step in the formation of the core oligosaccharide deployed in N-linked glycosylation. The transfected protoplasts were visualized with CSLM 12 hours after the transfection. The localization of AtSERK1-YFP in tunicamycin-treated protoplasts (Figure 5(b)) showed reduced membrane targeting of the

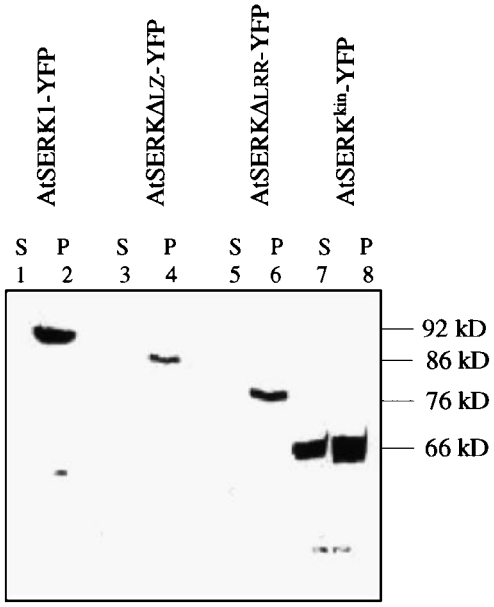


**Figure 2.** Immunoblot of AtSERK1 fusion proteins in transfected protoplasts. The protoplasts were harvested after 12 hours of transfection with AtSERK1-YFP transgenes, lysed and separated on a reducing SDS-10% PAGE. Proteins transferred to nitrocellulose paper were immunoblotted with anti-GFP antibody. S and P denote the soluble cytosolic fractions and the insoluble pellet fractions respectively. Lanes 1 and 2: AtSERK1-YFP; lanes 3 and 4: AtSERK1ΔLZ-YFP; lane 5 and 6: AtSERK1ΔLRR-YFP; lane 7 and 8: AtSERK1$^{kin}$-YFP. The molecular mass of the proteins is indicated in kDa.

AtSERK1 protein and increased intracellular clogging similar to that observed with the truncated AtSERK1ΔLRR-YFP protein (Figure 4(e) and (f)) when compared with untreated protoplasts (Figure 5(a)). Pretreatment of AtSERK$^{ins}$-CFP-YFP expressing insect cells with 20 μg ml$^{-1}$ of tunicamycin also showed intracellular clogging in vesicles (results not shown) comparable to tunicamycin-treated plant protoplasts. Proteins from tunicamycin-treated and untreated AtSERK$^{ins}$-CFP-YFP expressing insect cells were isolated, separated by denaturing SDS-PAGE and immunoblotted using an antiserum against GFP. There was a reduction of the molecular weight of the AtSERK1$^{ins}$-CFP-YFP fusion protein from 96 kD to 84 kD in the tunicamycin treated cell extract when compared to the untreated AtSERK1$^{ins}$-YFP-CFP infected Sf21 cells (Figure 5(b)). These results suggest that AtSERK1 is glycosylated in both insect cells and cowpea protoplasts and that N-linked glycosylation may be important for targeting the AtSERK1 protein to the plasma membrane.

### Homodimerization of AtSERK1 protein: interaction in yeast

To determine if the AtSERK1 receptor was capable of forming homodimers, the AtSERK1 intracellular kinase domain (AtSERK1$^{(266-625)}$), the extracellular domain (AtSERK1$^{(26-234)}$) and the AtSERK1 protein without signal sequence (AtSERK1$^{(31-625)}$) were fused to the B42 activation domain (AD) in pJG4-5 and the lexA DNA-binding domain (BD) in pEG202 (Figure (1)(v, x)). There was no interaction between the two intracellular kinase domains of AtSERK1 (AtSERK1$^{(266-625)}$ in Figure 6) whereas the AtSERK1 extracellular domains do interact with each other (AtSERK1$^{(26-234)}$ in Figure 6) as indicated by the β-galactosidase activity and the growth without leucine. The interaction, between two full-length AtSERK1 proteins lacking the N-terminal signal sequence was slightly reduced compared to the interaction shown by the extracellular domains only (AtSERK1$^{(31-625)}$ in Figure 6). This is most likely due to aberrant folding of the full-length membrane receptor protein in the yeast nucleus. From these data we conclude that the AtSERK1 extracellular domains are

**Figure 1.** AtSERK1 constructs used in this study. Different domains of (a) AtSERK1 and (b)-(q) AtSERK1 fusion constructs used for expression in plant protoplast, (r)-(x) yeast two hybrid studies and (y) expression in Sf21 insect cells are shown. The AtSERK1-YFP/CFP transgenes were constructed in the PMON999 vector under control of the 35 S promoter. (b) and (c) AtSERK1-YFP/CFP contains cDNA encoding for the full-length AtSERK1 as a C-terminal fusion with the YFP/CFP genes. (d) and (e) AtSERK1$^{kin}$-YFP/CFP encodes only the intracellular kinase domain of AtSERK1 fused to YFP/CFP. The truncated constructs, (f) and (g) AtSERK1ΔLZ-YFP/CFP and (h) and (i) AtSERK1ΔLRR-YFP/CFP were constructed by removing the leucine zipper and the five extracellular LRRs respectively from the coding sequence of ArSERK1. A series of LRR truncated constructs was made by removing LRRs starting from the N-terminal end and fusing the rest of the coding sequence of AtSERK1 to the YFP. This resulted in the construction of (j) AtSERK1ΔLRR$^{1}$-YFP, (k) AtSERK1ΔLRR$^{1,2}$-YFP, (l) AtSERK1ΔLRR$^{1,2,3}$-YFP, and (m) AtSERK1ΔLRR$^{1,2,3,4}$-YFP. (n) and (o) EGFR$^{3x}$-AtSERK1$^{kin}$-YFP/CFP chimeras were constructed by fusing the extracellular domain of EGFR and the intracellular kinase domain of AtSERK1-YFP/CFP. A single mutation in the AtSERK1 extracellular domain just above the transmembrane domain resulted in (p) and (q) AtSERK1$^{Y230C}$-YFP/CFP constructs. An AtSERK1 (amino acid residues 31 to 625) construct lacking only the N-terminal signal sequence, and AtSERK1 constructs consisting of the extra-cellular domain or the intracellular domain only were fused to the activation domain (AD: pJG 4-5) or to the LexA DNA-binding protein (BD: pEG202) resulted in (r) and (s) AtSERK1$^{(31-625)}$-BD/AD, (t) and (u) AtSERK1$^{(26-234)}$-BD/AD, (v) and (x) AtSERK1$^{(266-625)}$-BD/AD. For expression in insect cells the full length AtSERK1 fused to YFP and the full-length AtSERK1 fused to CFP were cloned in front to the viral p10 and polyhedrin promoters respectively resulting in the (y) AtSERK$^{ins}$-CFP/YFP.

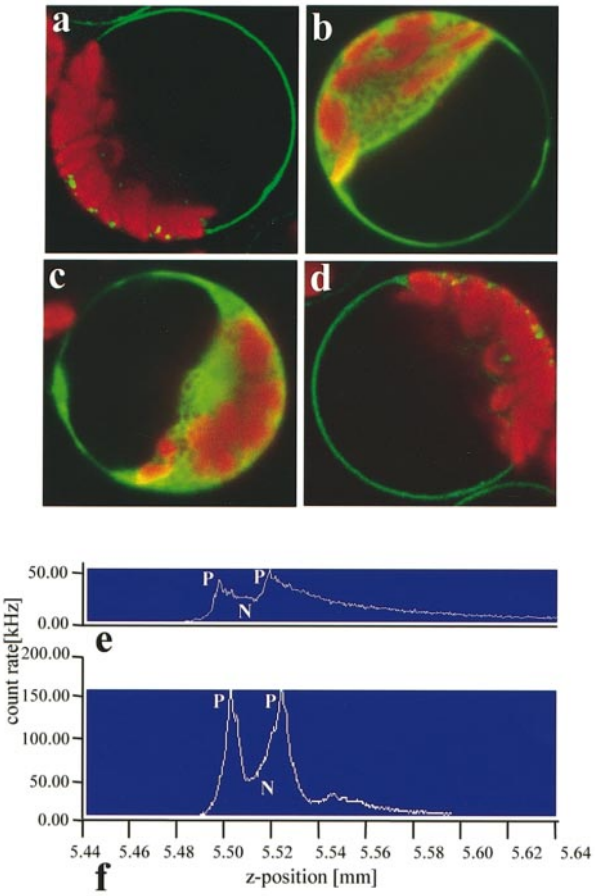


**Figure 3.** Confocal fluorescence images of protoplasts transfected with. (a) AtSERK1-YFP, (b) PMON999-YFP, (c) AtSERK1$^{kin}$-YFP, (d) EGFR$^{ex}$-AtSERK1$^{kin}$-YFP. In green the YFP fluorescence is shown and in red the chlorophyll fluorescence is shown. (e) and (f) Fluorescence correlation spectroscopy (FCS) of AtSERK1-YFP-CFP fusion proteins in insect cells. The profiles show the count rate along the optical *z*-axis of the (e) non-infected cells and the (f) AtSERK1-YFP expressing Sf21 cells. N and P indicate the fluorescence recorded in the nucleus and the plasma membrane, respectively.

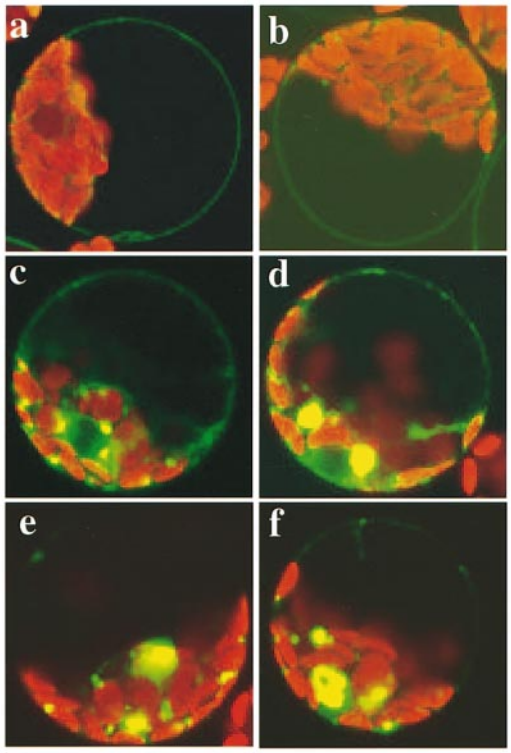


**Figure 4.** Confocal fluorescence images of protoplasts transfected with LZ and the series of LRR truncated constructs: (a) AtSERK1ΔLZ-YFP, (b) AtSERK1ΔLRR$^{1}$-YFP, (c) AtSERK1ΔLRR$^{1,2}$-YFP, (d) AtSERK1ΔLRR$^{1,2,3}$-YFP and (e) AtSERK1ΔLRR$^{1,2,3,4}$-YFP and (f) AtSERK1ΔLRR-YFP expression is shown. In green the YFP fluorescence is shown and in red the chlorophyll fluorescence is shown.

capable of homodimerization while the kinase domains are unlikely to interact physically.

### Oligomerization of the AtSERK1 protein: fluorescence energy resonance transfer between CFP and YFP

Because protein-protein interactions demonstrated in the yeast system may not be representative of interactions in living plant cells, nor for interactions in membranes, we used cowpea protoplasts coexpressing AtSERK1-CFP and AtSERK1-YFP fusion proteins. Possible AtSERK1 dimerization was then studied by measuring FRET between the CFP (donor) and the YFP (acceptor) fluorophores. All experiments were based on fluorescence spectral imaging microscopy (FSPIM) as a detection system. Spectral images were taken from plasma membrane-regions of protoplasts coexpressing AtSERK1-YFP and AtSERK1-CFP and a fluorescence emission spectrum corrected for background fluorescence was then generated. In case of FRET, the CFP fluorescence will be quenched and the YFP fluorescence would be increased (sensitized). Assuming approximately equal expression levels of both AtSERK1-CFP (Figure 1(c)) and -YFP (Figure 1(d)), we consider a ratio of fluorescence intensity at 525 nm over 475 nm (designated as the YFP/CFP emission ratio) of 1.3 or higher as evidence of FRET and hence of AtSERK1-AtSERK1 interactions such as oligomerization or homodimerization. It should be emphasized that with the FSPIM technique it cannot be resolved whether the nonmonomeric AtSERK1-receptors are dimeric, trimeric or present as higher oligomeric structures.

A single protoplast coexpressing AtSERK1-CFP and AtSERK1-YFP fusion proteins is shown in Figure 7(a). Five areas of which spectral images are recorded are indicated by rectangles. The YFP/CFP emission ratios deduced from these spectra is close to 1.0 in four of the five measurements and

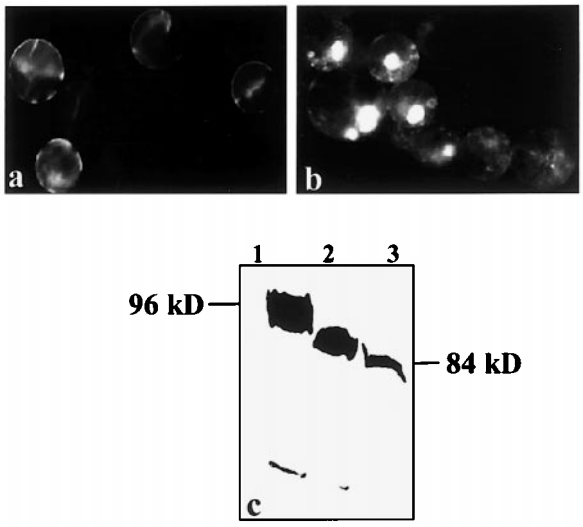


**Figure 5.** The effect of tunicamycin on protoplasts and Sf21 cells expressing AtSERK1-YFP. (a) Protoplasts transfected with AtSERK1-YFP and visualized after 12 hours of transfection. (b) Protoplasts treated with 20 μg $ml^{-1}$ of tunicamycin three hours after transfection with AtSERK1-YFP and visualized after 12 hours of transfection. (c) Immunoblot analysis of the Sf21 insect cells, untreated (lane 1) and treated with either 10 μg $ml^{-1}$ (lane 2) or 20 μg $ml^{-1}$ (lane 3) of tunicamycin prior to $AtSERK1^{ins}$-CFP-YFP infection, harvested after 48 hours, lysed and separated on reducing SDS-8% PAGE. Proteins were transferred to nitrocellulose paper and immunoblotted with anti-GFP antibody. The molecular mass of the proteins is indicated in kDa.

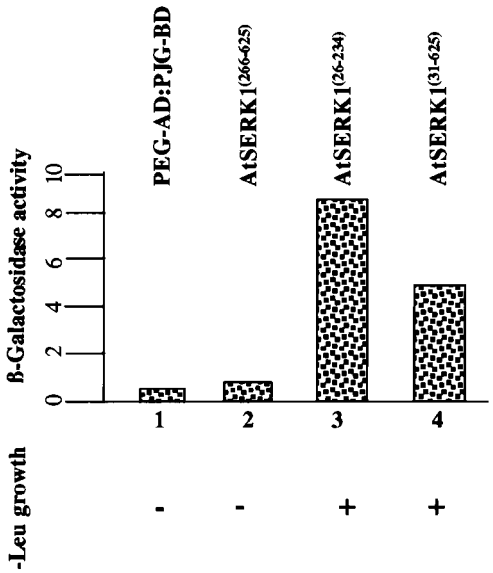


**Figure 6.** AtSERK1-AtSERK1 interactions in yeast using lexA two-hybrid vectors. The $AtSERK1^{(31-625)}$, $AtSERK1^{(26-234)}$, $AtSERK1^{(266-625)}$ fused to the activation domain (AD: pJG 4-5) or with the LexA DNA binding protein (BD: pEG202) were transformed into yeast strain EGY 48 and β-galactosidase activity and growth on leucine was determined.

1.35 in only one measurement (Figure 7(c)). Repeating this experiment in ten different protoplasts and taking five measurements from each protoplast revealed that the YFP/CFP emission ratio is close to 1.0 in about 80% of the spectral measurements and 1.35 in 15% of the measurements. This indicates that receptor oligomerization is not uniformly distributed within the membrane of a single protoplast. The percentage of YFP/CFP emission ratios deduced from single spectral measurements on 60 protoplasts co-expressing AtSERK1-CFP and AtSERK1-YFP are shown in Figure 7(e). About 15% of the measurements show an increased YFP/CFP emission ratio of 1.35, which is similar to the results obtained from a single protoplast (Figure 7(c)). The protoplasts co-expressing the intracellular $AtSERK1^{kin}$-CFP (Figure 1(e)) and $AtSERK1^{kin}$-YFP (Figure 1(d) and Figure 7(b)) showed no or little increase in YFP (acceptor) fluorescence (Figure 7(d)). The YFP/CFP emission ratio was close to 1.0 in all five measurements was recorded from the different points (shown by rectangles) in the protoplast (Figure 7(b)). Repeating this experiment in ten different protoplasts and taking five measurements from each protoplast revealed a YFP/CFP emission ratio close to 1.0 in about 95% of the spectral measurements. Similar results were obtained when single spectral measurements were performed on 60 protoplasts coexpressing $AtSERK1^{kin}$-CFP and $AtSERK1^{kin}$-YFP (Figure 7(e)). Collectively, these results show that in the protoplasts analyzed, most of the AtSERK1 receptor molecule (~85%) are in the monomeric state while up to 15% may be oligomerized. No interaction was found between the kinase domains expressed in the cytoplasm, which confirms the yeast two-hybrid experiments.

The YFP/CFP emission ratios as shown in Figure 7 may suffer from several potential artifacts, an unbalanced expression ratio of the donor and the acceptor fluorophores or the absorption of the CFP fluorescence by chlorophyll in plant cells. To exclude the first possibility, we performed more than ten independent transfection experiments in which we coexpressed AtSERK1-CFP and AtSERK1-YFP fusion proteins. In each of these transfections 80% of the protoplasts exhibited a constant YFP/CFP emission ratio indicating a constant expression ratio. In addition, the variation in the YFP/CFP emission ratio within the same cell (in 15% of the cells) indicates that another phenomenon than an unbalanced expression ratio must be responsible for enhanced YFP/CFP emission ratio (i.e. FRET). To avoid the second artifact, FSPIM measurements were performed exclusively over areas lacking chloroplasts. We therefore consider it likely that the results showing an increased donor/acceptor ratio are due to FRET between the CFP and the YFP molecules fused to the AtSERK1

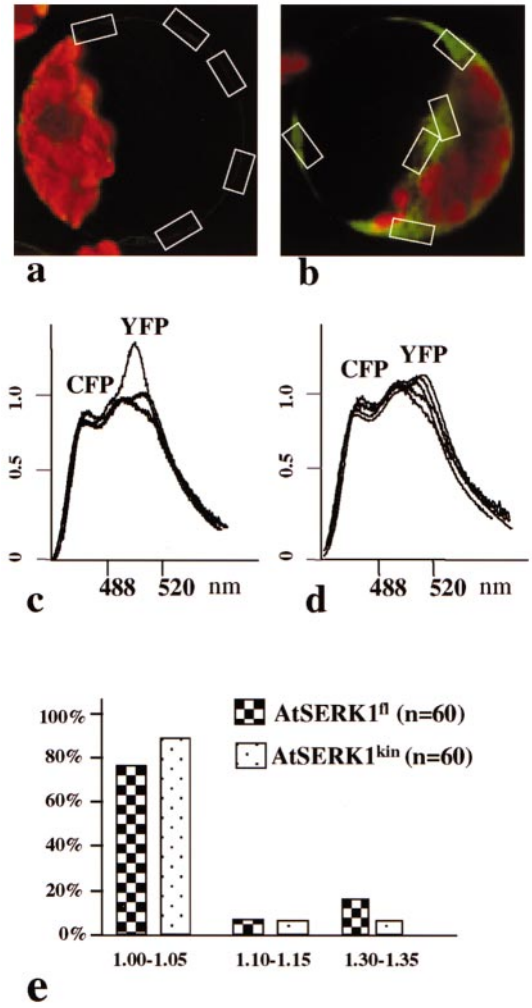


**Figure 7.** FSPIM analysis of fluorescent AtSERK1 fusion proteins. (a) Confocal image of a protoplast cotransfected with AtSERK1-YFP/CFP showing typical regions (rectangles) used for spectral measurements. (c) Emission spectra of the AtSERK1-CFP/YFP proteins obtained from the spectral images shown in (a). The *x*-axis represents wavelength (nm) and the *y*-axis represents the CFP and YFP fluorescence intensities. (b) and (d) The same for AtSERK1$^{kin}$-CFP/YFP, expressing protoplasts. (e) Comparison of the 525/475 nm fluorescence emission ratio (the YFP/CFP ratio), varying form 1.00 to 1.35, of the 60 protoplasts cotransfected with AtSERK1-CFP/YFP, and the protoplasts cotransfected with AtSERK1$^{kin}$-CFP/YFP.

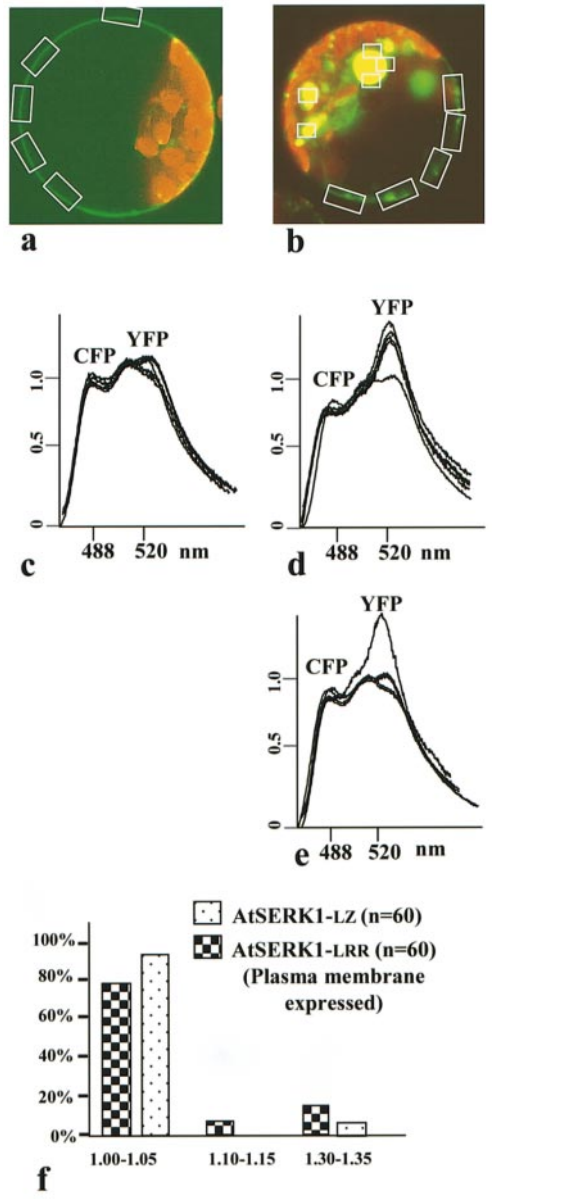


**Figure 8.** FSPIM analysis of truncated fluorescent AtSERK1 fusion proteins. (a) Confocal image of a protoplast cotransfected with AtSERK1ΔLZ-CFP/YFP showing typical regions (rectangles) used for spectral measurements. (c) Emission spectra of the AtSERK1ΔLZ-CFP/YFP proteins obtained from spectral images shown in (a). The *x*-axis represents wavelength (nm) and the *y*-axis represents the CFP and YFP fluorescence intensities. (b) Confocal image of a protoplast cotransfected with AtSERK1ΔLRR-CFP/YFP showing typical plasmamembrane regions (rectangles) and intracellular regions (small rectangles) used for spectral measurements and (d) emission spectra of the AtSERK1ΔLRR-CFP/YFP proteins obtained from plasma membrane regions, (e) Emission spectra of the AtSERK1ΔLRR-CFP/YFP proteins obtained from intracellular regions. (f) Comparison of the fluorescence emission ratio (YFP/CFP ratio) on the plasma membrane, varying from 1.00 to 1.35, of the 60 protoplasts cotransfected with AtSERK1ΔLZ-CFP/YFP, and the protoplasts cotransfected with AtSERK1ΔLRR-CFP/YFP.

protein, indicating receptor-oligomerization (e.g. homodimerization).

To verify whether AtSERK1 receptor oligomerization was dependent on the extracellular domains, protoplasts were co-transfected with AtSERK1ΔLZ-YFP (Figure 1(f)) and AtSERK1ΔLZ-CFP (Figure 1(g)) (Figure 8(a)). Experiments were performed in the same way as described for the full-length AtSERK1 receptor as shown in Figure 7. The spectra obtained from the area of the protoplast expressing AtSERK1ΔLZ-YFP and

AtSERK1ΔLZ-CFP (Figure 8(a)) at the plasma membrane (indicated by rectangles) showed that there was no increase in YFP fluorescence in almost all the measurements recorded (Figure 8(c)). Repeating this experiment in ten different protoplasts taking five measurements from each protoplast revealed that the intensity ratio is close to 1.0 in about 95% of the spectral measurements. The same results were obtained when single spectral measurements were performed on 60 co-expressing AtSERK1ΔLZ-CFP (Figure 1(i)) and AtSERK1ΔLZ-YFP protoplasts (Figure 8(f)). Next, protoplasts co-expressing AtSERK1ΔLRR-CFP and AtSERK1ΔLRR-YFP (Figure 1(h) and Figure 8(b)) were analyzed. The FSPIM measurements on protoplast expressing these truncated AtSERK1 receptors were performed on both types of receptor molecules, the ones that were properly targeted to the plasma membrane (shown by rectangles) and the ones that remained clogged in the intracellular vesicles (shown by small rectangles) (Figure 8(b)). The spectra derived from the five measurements on areas indicated by small rectangles showed an increased fluorescence ratio of 1.35 in three to four out of five measurements (Figure 8(d)). When this experiment was repeated in ten different protoplasts, there was an increase YFP/CFP of 1.35 in 70% of the measurements recorded. A YFP/CFP fluorescence intensity ratio close to 1.35 was seen in 1 out of 5 measurements recorded from the different points indicated by rectangles at the plasma membrane of the protoplast. Repeating this experiment in 10 different protoplasts showed that about 15% of the measurements had an increased ratio of 1.35 (Figure 8(e)). When these experiments were performed at the plasma membrane of 60 different protoplasts taking one single measurement from each protoplast, the results coincided with the measurements shown for each individual protoplast (Figure 8(f)). The results show that there was an increased YFP/CFP fluorescence intensity ratio again in about 15% of the coexpressing protoplasts suggesting that LRRs are not involved at all in AtSERK1 dimerization at the plasma membrane.

To determine whether AtSERK1 receptor-dimerization at the plasma membrane could be increased by an intermolecular disulfide bond, we introduced a single unpaired cysteine in the extracellular domain in the region immediately adjacent to the transmembrane domain (Y230C). Protoplasts cotransfected with AtSERK1$^{Y230C}$-YFP and AtSERK1$^{Y230C}$-CFP constructs (Figure 1(p) and (q)) showed protein localization similar to that of AtSERK1-YFP and AtSERK1-CFP (results not shown). The spectra from these protoplasts were obtained in the same way as for AtSERK1-YFP and AtSERK1-CFP. In about 15% of the measurements, the YFP/CFP ratio increased to 1.35 (Figure 9). Since this is similar to the ratio observed in full length AtSERK1 proteins, the introduction of an extra cysteine residue does not appear to result in increased AtSERK1 receptor dimerization.

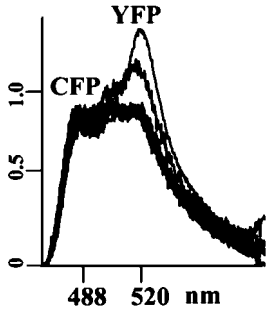


**Figure 9.** FSPIM analysis of truncated fluorescent AtSERK1 fusion proteins. Emission spectra of the AtSERK1$^{Y230C}$-CFP/YFP proteins after excitation at 430 nm.

The synthetic auxin 2,4-dichlorophenoxy acetic acid (2,4-D) is commonly used to initiate somatic embryogenesis. Because of the correspondence between the acquistion of embryogenic potential and SERK expression[21] we investigated if 2,4-D itself can influence AtSERK1 dimerization. Protoplasts were cotransfected with AtSERK-CFP and AtSERK-YFP and were treated with 2,4-D. There was no change in the YFP/CFP emission ratio at the plasma membrane (data not shown).

Taken together, we conclude from these results that the predominant form of AtSERK1 is monomeric and that up to 15% of the AtSERK1-CFP/YFP proteins may be oligomerized (possibly as homodimers) at the plasma membrane of the protoplasts. The oligomerization appears to require only the extracellular LZ domain and not the LRRs or the kinase domain of AtSERK1.

## Discussion

The major goals of this work were to determine the subcellular localization of the AtSERK1 protein and to determine whether the AtSERK1 protein was capable of homodimerization *in vivo*. The results show that AtSERK1 is a plasma membrane protein that occurs predominantly as a monomer. In living plant cells, less than 15% of the receptor molecules may exist as a homodimer.

Based on the cDNA sequence, the AtSERK1 protein was predicted to be a membrane associated serine/threonine receptor protein kinase (V. Hecht *et al.*, unpublished results). This prediction was supported by several experiments. Western blot analysis showed that AtSERK1-YFP fusion proteins produced in plant protoplasts are present in a 40,000 *g* pelletable cell fraction whereas similar YFP fusion proteins lacking the extracellular and transmembrane domains remained in the soluble fraction. Confocal microscopy with AtSERK1-YFP expressed in plant protoplasts showed the presence of the fusion proteins in the plasma membrane in a pattern comparable with that of an EGFR$^{ex}$-AtSERK1$^{kin}$-YFP chimeric protein. Finally, FCS

indicated that the AtSERK1-YFP fusion protein was located in the plasma membrane of insect cells. Based on these data we propose that the functional AtSERK1 receptor kinase is located in the plasma membrane.

The correct assembly and localization into the plasma membrane of a glycosylated receptor kinase such as AtSERK1 must involve a series of events. The AtSERK1 predicted proprotein has a 29 amino acid signal sequence, immediately followed by the LZ domain and the five LRRs (V. Hecht *et al*., unpublished results). Thus, it is likely that the protein is synthesized on the ER membrane and translocated into the ER lumen where *N*-glycosylation of the LRRs takes place. The extracellular domains of most of the characterized transmembrane receptors have been shown to be involved in ligand binding, oligomerization and the subsequent activation of the intracellular kinase domain and the initiation of the downstream signal transduction cascade.[4] More recently, it is becoming clear that the extracellular domains are also involved in correct targeting of the receptors. For instance, the correct folding, assembly and expression of the human insulin receptor depends on glycosylation of the extracellular domains.[20] Inhibition of N-linked glycosylation by tunicamycin leads to the intracellular accumulation of non-glycosylated insulin proreceptors, that fail to fold correctly.[37] The LRRs of AtSERK1 contain five putative N-glycosylation sites. Two of these are present in the second LRR, two in the fourth and one in the fifth LRR starting from the N terminus of the AtSERK1 protein. Removal of at least two of the LRRs resulted in considerable reduction of the number of AtSERK1 protein molecules being targeted to the plasma membrane. In line with the role of N-linked glycosylation in insulin receptor targeting, AtSERK1 mistargeting would be due to the lack of glycosylation of the extracellular LRRs. Support for this hypothesis comes from tunicamycin studies suggesting a role of the N-linked glycosylation in AtSERK1 protein targeting to the plasma membrane.

Several roles of addition of N-linked oligosaccharides to nascent proteins have been demonstrated; for example, N-linked oligosaccharides attach to lectin-like molecular chaperones such as calnexin and calreticulin,[19] facilitating correct protein folding.[38] N-linked oligosaccharides also play a role in the ''quality control'' system of the ER that ensures selective transportation of the properly folded proteins destined for the Golgi complex.[39] Removal of the N-linked oligosaccharides either by chemical means or through removal of LRRs may thus result in incorrectly folded, non-glycosylated AtSERK1 proteins and these may be trapped in the ER. This suggests that recognition of properly glycosylated proteins by an ER-based sorting machinery is an essential element of the assembly and localization process.

Receptor dimerization is employed as a mechanism for both receptor activation and autophosphorylation.[8,40] Well-known examples are the epidermal growth factor receptor (EGFR) and platelet derived growth factor receptor (PDGFR) that undergo dimerization in response to binding of their respective ligands. However, the sensitivity of the PDGFR[41] and some other receptors like calcium sensing receptor (CaR)[42] to reducing agents suggests that one type of intermolecular interaction mediating dimerization is *via* intermolecular disulfide bonds.

The mechanism by which plant receptors transduce signals across the cell surface is largely unknown. There is evidence which suggests that plant receptors like CLV1 and CLV2 also dimerize[12] and are assembled into a heterodimeric complex to transduce extracellular signals.[15] Recent studies have shown that CLV1 and CLV3 form a potential receptor/ligand pair and that CLV3 binds to the CLV1 and CLV2 heterodimer to form a multimeric protein complex.[16]

Our experiments suggest that the AtSERK1 receptor can form oligomerized structures such as homodimers. This is based both on yeast interaction experiments and expression of AtSERK1-CFP/YFP fusion proteins in protoplasts. In the latter studies, one potential problem may be that AtSERK1 expression is raised far beyond normal levels due to the use of the strong constitutive 35 S promoter. However, because the majority of the protoplasts expressing AtSERK1 fusion proteins do not show FRET and therefore exist as monomers in the membrane, this does not appear to be a wide spread problem. It also appeared that there are only certain regions on the plasma membrane where AtSERK1 is not monomeric. This could indicate that a minority of AtSERK1 receptor molecules on the plasma membrane is in a predimerized state. This observation is in line with EGF receptor dimerization in mammalian cells. High affinity EGF receptors (12 %) dimerize highly in some regions of the plasma membrane. Based on the quantitative determination of FRET on the EGF receptor in mammalian cells, it was suggested that the high affinity subclass of receptors are present in a predimerized state in the absence of the ligand.[36] The predimerized AtSERK1 receptor molecules on the plasma membrane appear to be far less abundant than those observed for the EGF receptor owing to the fact that in only one out of five measurements, there appeared to be a change in the fluorescence intensity ratio. In addition, the ratio change is on the lower side of FRET detectability. This also indicates that the region of the plasma membrane used for single FRET measurements (indicated by rectangles in Figure 7 and Figure 8) mainly contain AtSERK1 receptors that are in the monomeric form. The small population of non-monomeric AtSERK1 receptors are not detected in the absence of the LZ domain in the AtSERK1 receptor, implying that our FSPIM detection system is sensitive enough to detect the change from a fully monomeric to a state

where monomeric and oligomeric AtSERK1 receptor coexist.

LZ domains have been shown to play a role in dimerization of various nuclear and cytoplasmic proteins such as Nek2,[43] ZIP kinases,[44] MLK-3[45] and TSC-22,[46] respectively. There are also recent reports that show the involvement of the LZ domain in receptor dimerization.[47] The presence of cysteines in the N-terminal extracellular domains of transmembrane receptors has been shown to have a role in receptor dimerization by the formation of disulfide bridges.[48] In animals, the type II transforming growth factor receptor (also a receptor serine/threonine kinase) can form homodimers in the absence of ligands,[49,50] whereas the insulin growth factor receptor is found as a disulfide-linked tetramer.[51] Since it is not known whether ligands that bind to AtSERK1 are present in the protoplast culture medium, we cannot answer whether the putative AtSERK1 dimers detected by FSPIM represent ligand-activated dimers or preassociated dimers. The presence of conserved cysteine pairs in the extracellular domains of plant RLKs may imply that a population of predimerized receptors on the cell surface can exist.[52] Among plant RLKs, CLV1 and CLV2 form a disulfide linked heterodimeric receptor complex[15] and also the ethylene receptor, ETR1, is a disulfide linked dimer.[53] The SRG protein involved in the pollen recognition in *Brassica* stigma is also found as a disulfide-linked dimer.[54] The AtSERK1 protein has four cysteine residues in the extracellular domain so the small amount of AtSERK1 oligomers found might arise due to the formation of disulfide bridges between the cysteines in the LZ domain. Generation of stable disulfide-bonded receptor-like-protein tyrosine phosphatase-α, (RTPT-α) homodimers by introducing a single cysteine in the extracellular domain immediately adjacent to the transmembrane domain has been shown.[55] The introduction of a cysteine residue in a comparable region as RTPT-α does however not change the oligomerization state of the AtSERK1 receptor, so disulfide linkages may be of less importance in AtSERK1 homodimerization.

While identification of the ligand for AtSERK1 is clearly essential for determining its precise mode of action, we propose that AtSERK1 exhibits ligand-induced homodimerization which would place it in the EGF class of receptors.

## Materials and Methods

### AtSERK1-YFP/CFP tagged vectors

The entire open reading frame of the *AtSERK1* cDNA was amplified by PCR from a *AtSERK1* full-length cDNA (acc. no: A67827) and cloned downstream of the 35 S promoter into the *Nco*I site of pMON999-CFP and pMON999-YFP using primers *Nco*I215f 5′ CATGCCATGGTGGAGTCGAGTTATGTGG 3′ and *Nco*I2068r 5′ CATGCCATGGACCTTGGACCAGATAACTC 3′. This clone and all subsequently described clones are shown schematically in Figure 1. The AtSERK1 intracellular kinase domain was similarly cloned into the *Nco*I site of pMON999-CFP and pMON999YFP using primers nAtSERKC 5′ CCATCCGATGGGCCCACTAGATATTT TCTT 3′ and *Nco*I2068r. This resulted in the fusion constructs AtSERK1-YFP;AtSERK1-CFP (Figure 1(b) and (c)) and AtSERK1$^{kin}$-YFP;AtSERK1$^{kin}$-CFP (Figure 1(d) and (e)). A 60-bp *Noc*I-*Kpn*I fragment DyiiKgPSp *Kpn*I-*Noc*I fragment corresponding to the coding sequence of the AtSERK1 cDNA without the leucine zipper were prepared by PCR using primer pair *Nco*I215 and *Kpn*I260 5′ CAAATTAGCAGAAGCAAGCCAC 3′ and primer pair *Kpn*I420 5′ TGGGGAATGCAGAGTTATCTGGC 3′ and *Nco*I2068, respectively. Both were ligated into the *Nco*I site of PMON999-CFP/YFP plasmids to create truncated AtSERK1 fusion constructs without the leucine zipper domain. The fusion constructs were named AtSERK1ΔLZ-CFP and AtSERK1ΔLZ-YFP (Figure 1(f) and (g)). To create the truncated AtSERK1 fusion constructs (without the extracellular LRRs), the AtSERK1-CFP and YFP constructs were digested with *van91* and religated, resulting in AtSERK1ΔLRR-YFP and AtSERK1ΔLRR-CFP constructs (Figure 1(h) and (i)). A series of constructs with one or more LRRs deleted were prepared by PCR. DNA fragments of 1580-bp (primers *Kpn*I489 5′ CGGGGTACCGAGCTTTACAGTAACAACATAAC 3′ and *Nco*I2068r), 1508 bp (primers *Kpn*I561 5′ CGGGGTACCGATCTTTACTTAAACAGCTTCT 3′ and *Nco*I2068r), 1364-bp (primers *Kpn*I633 5′ CGGGGTA CCCGGCTTAACAACAACAGTCT 3′ and *Nco*I2068r), and 1292-bp (primers *Kpn*I705 5′ CGGGTACCGATCTATCAAATAACAGACTCT 3′ and *Nco*I12068r) generated with 5′ *Kpn*I and 3′ *Nco*I linkers were prepared by PCR. They were ligated together with a 60-bp *Nco*I-*Kpn*I fragment corresponding to the signal sequence of AtSERK1 cDNA into the *Nco*I site of pMON999-YFP plasmids. This resulted in the series of truncated AtSERK1 fusion constructs designated as AtSERK1ΔLRR$^{1}$-YFP (Figure 1(j)), AtSERK1ΔLRR$^{1,2}$-YFP (Figure 1(k)), AtSERK1ΔLRR$^{1,2,3}$-YFP (Figure 1(l)) and AtSERK1ΔLRR$^{1,2,3,4}$-YFP (Figure 1(m)), respectively.

A 2.1-kb *Bgl*II/*Nco*I fragment corresponding to the extracellular and transmembrane domain of human EGFR was amplified by PCR using primers EGFBglIIf 5′ GGAAGATCTGCGATGCGACCCITCCGGG 3′ and EGFNcoIr 5′ CATGCCATGGGGCGCTTCCGAACGATGTGG 3′ and ligated into the *Bgl*II/*Nco*I sites of PMON999-CFP/YFP vectors. The resulting plasmids were digested with *Nco*I and the *Nco*I/*Nco*I fragment encoding the AtSERK1 intracellular kinase domain was cloned in frame with the C-terminus of EGFR cDNA. This resulted in EGFR$^{ex}$-AtSERK1$^{kin}$-YFP/EGFR$^{ex}$-AtSERK1$^{kin}$-CFP chimeras (Figure 1(n) and (o)).

For expression in insect cells a Pdual Fast Bac vector, that contains a polyhedrin and a p10 promoter was used. The entire coding sequence of the AtSERK1-CFP using primers KCNot1 5′ ATAAGAATGCGGCCGCGGATCCTTACTTGTACAGCTCG 3′ and KCSa1I 5′ ACGCGTCGACAGAGCCATGGTGGAGTCGAG 3′ and the AtSERK1-YFP fusion using primers KYKpnI 5′ CGGGGTACCGGATCCTTACTTGTACAGCTCG 3′ and KYSmaI 5′ TCCCCCGGGAGAGCCATGGTGGAGTCGAG 3′ were amplified by PCR and cloned into the *Sma*I/*Kpn*I sites downstream of the polyhedrin promoter and *Sal*I/*Not*I sites downstream of the p10 promoter respectively. This resulted in the AtSERK1$^{ins}$-CFP-YFP construct (Figure 1(g)). All the constructs were confirmed by sequence analysis.

### Site-directed mutagenesis

This fusion constructs AtSERK1-YFP and AtSERK1-CFP were used for replacing tyrosine230 with single unpaired cysteine230 in the extracellular domain immediately adjacent to the transmembrane domain. Site directed mutagenesis was performed according to manufacturer's instructions (Stratagene). This resulted in the AtSERK1$^{Y230C}$-YFP and AtSERK1$^{Y230C}$-CFP (Figure 1(p) and (q)) constructs. Clones incorporating the mutations were confirmed by DNA sequence determination.

### Transient expression in protoplasts

Cowpea mesophyll protoplasts were prepared essentially as described by Rezelman *et al*.[56] except that 10 mM $CaCl_2$ was added to the enzyme solution (0.5 M mannitol, 10 mM $CaCl_2$, 0.1 % cellulase and 0.05 % pectinase). Ten to fifteen micrograms of each purified plasmid DNA in 20-75 µl of water was added to 0.5-1 $\times$ $10^6$ protoplasts in 75-150 µl of ice cold solution C (0.6 M mannitol, 10 mM $CaCl_2$ (pH 5.3-5.8), mixed by gentle shaking and followed immediately by the addition of solution H (40 % (w/v) PEG Mw 6000, 0.6 M mannitol, 0.1 M $Ca(NO_3)_2$. The protoplast suspension was incubated for 5-25 seconds with gentle shaking followed by the addition of 4.5 ml of solution M (0.5 M mannitol, 15 mM $MgCl_2$ and 0.1 % MES (pH 5.3-5.7) and incubated at room temperature for 20 minutes. Protoplasts were then washed 3 times with solution M and incubated for 8-24 hours as described by Rottier *et al*.[57] For glycosylation studies, protoplasts were treated with 20 µg ml$^{-1}$ of tunicamycin three hours after transfection. Protoplasts were mounted on microscopic slides and visualized under fluorescence microscope. For dimerization studies with 2,4-D, cotransfected protoplasts were treated with 2 µM 2,4-D 12 hours after transfection.

### Expression in insect cells

Monolayers of Sf2l cells ($1 \times 10^6$ cells/35 mm Petri dish) were cotransfected with 2 µg of recombinant plasmid DNA (obtained by transforming DH10BAC *Escherichia coli* cells (GIBCO-BRL)) with AtSERK1$^{ins}$-CFP-YFP Pdual FastBac plasmid DNA using a lipofectin reagent (GIBCO-BRL) as described.[58] After 72 hours of incubation in Graces's medium (GIBCO-BRL) at 27 °C, the supernatant containing extracellular virus particles was collected and Sf21 cell monolayers were infected. For glycosylation studies in insect cells, the tunicamycin treatment was performed on cells prior to the infection with recombinant AtSERK1$^{ins}$-CFP-YFP virus.

### SDS PAGE and Western Blotting

Twelve hours (cowpea protoplasts) or two to three days (insect cells) after transfection, cells were lysed in ice cold HB buffer (50 mM Tris-HCl (pH 7.4), 10 mM KAc, 1 mM EDTA) supplemented with single strength proteinase inhibitor cocktail (Boehringer). The lysates were passed through a 25 µm needle and centrifuged at 40,000 *g* for 30 minutes 4 °C. Thirty microlitre of 2$\times$ SDS sample buffer (100 mM Tris HCl(pH 6.8), 4 % (w/v) SDS, 0.2 % (w/v) bromophenol blue and 20 % glycerol) and DTT was added to lysates as well as to pellets. After boiling for three minutes, the proteins were separated by SDS-PAGE and transferred to nitrocellulose membrane (IMMOBILON) for three hours at 50 V. The membranes were washed in TBS-T buffer (10 mM Tris-HCl (pH 7.5), 150 mM NaCl, 0.2 % (v/v) Tween-20) and blocked with 5 % (w/v) non-fat dried milk in TBS-T with for three hours at room temperature, washed with TBS-T and incubated with the anti-rabbit GFP antibody (Clontech; 1:100 final dilution) for 1.5 hours at room temperature. After three washes in TBS-T, membranes were incubated with alkaline phosphatase conjugated anti-rabbit antibody (New England Biolabs; 1:1000 final dilution). Membranes were washed in TBS-T, incubated in Western blue substrate for Alkaline Phosphatase detection (Promega) until staining was visible.

### Construction and transformation of yeast two hybrid plasmid vectors

The coding sequence of AtSERK1 cDNA without signal sequence (spanning amino acid residues 31-625), the kinase domain (amino acid residues 266 to 625) and extracellular domain (amino acid residues 26 to 234) were cloned into either PEG202 bait or PJG4-5 prey yeast expression vectors to generate the translational fusions of AtSERK1 domains with either the *E. coli* peptide (B42) as activation domain (AD: pJG 4-5) or with the LexA DNA binding domain (BD: pEG202) obtained from the DuplexA two-hybrid system (Origene Technologies). All constructs were verified by sequence analysis and are shown in schematic form in Figure 1. Yeast (*Saccharomyces cerevisae*) strain EGY 48 (lacZ) was transformed with the plasmid constructs and an autoactivation assay and a repression assay of the AtSERK1 fusion constructs was performed according to the users manual to determine possible self-activation and proper entry of the proteins into the nucleus, respectively. Yeast cells cotransformed with both bait and prey constructs were grown at 30 °C for two days. Colonies obtained were scored as positive when they could grow in absence of leucine and show β-galactosidase activity within 72 hours at 30 °C.

### Confocal microscopy

Surface fluorescence and intracellular fluorescence was analyzed by confocal laser scanning microscopy (CLSM) using a Zeiss LSM 510 microscopy system (Carl-Zeiss) based on an Axiovert inverted microscope equipped with an Argon ion laser as excitation source. Protoplasts were excited at 514 nm and YFP fluorescence was separated from chlorophyll fluorescence by using a Zeiss 630 dichroic beamsplitter. YFP emission was selectively detected by using bandpass 535-590 nm filter, and chlorophyll fluorescence was detected simultaneously in another detection channel using a 650 nm longpass filter. A 40$\times$ oil immersion objective (numerical aperture 1.3) was used for scanning protoplasts with step (pixel) size of 0.2 µm$^2$ in the *xy* plane and a step size of 0.4 µm$^2$ for serial optical sections in the *z*-axis. The pinhole setting was 40 µm, which yielded a theoretical thickness (full width at half maximum) of approximately 1 µm.

### Fluorescence correlation spectroscopy

Three days after infection with AtSERK1$^{ins}$-CFP-YFP, measurements on Sf21 cells were performed with a Zeiss-Evotec ConfoCor® system based on an Axiovert 100 inverted confocal microscope (Carl-Zeiss). The sample was excited using an Argon ion laser (output 10 mW). The filter block consisted of a 514 (Δ5) exci-

tation filter, a 530 (Δ20) dichroic mirror and a 570 (Δ40) emission filter. The light was focused into the sample (stored in glass-bottomed 96-well plates [Polyfiltronics]) by a water-immersible objective lens (40 ×, N.A. 1.2). The emitted light passes a size-adjustable pinhole (diameter 40 μm) to reject out-of-focus light, and finally hit an avalanche photodiode. Profile scans along the optical (*z*) axis through the cells were carried out by piezo-driven movement of the objective lens (step size 5 μm $s^{-1}$). Profile scans through the Sf21 insect cells incubated with Bodipy-labeled lipids indicated the position of the plasma membrane and the nucleus in the profile scan.

### Fluorescence resonance energy transfer between AtSERK1-CFP and AtSERK1-YFP on membrane associated AtSERK1 receptors

FRET between the fluorescently labelled AtSERK1 receptors in the plasma membrane was measured by FSPIM.[59] Spectral imaging was done using a Leica DMR epifluorescence microscope equipped with a 250IS imaging spectrograph (Chromex) coupled to a CH250 CCD camera (Photometrics) incorporating a back-illuminated SIT502 chip with 512 × 512 24 μm square pixels. The excitation light source was a 100 W-mercury arc lamp coupled to an excitation filter wheel. Fluorescent spectral images were acquired using a 20× Plan Neofluar objective (NA 0.5), a bandpass excitation filter (Omega), a 430DCLP dichroic mirror (Omega) and a 455 longpass emission filter (Schott). Spectral images were acquired using a 150 groove/mm grating, set at a central wavelength of 500 nm and a slit width of 200 μm corresponding to 10 μm in the object plane. Typical exposure and CCD integration time was two to five seconds. Data processing and background subtraction was performed as described.[60]

## Acknowledgments

We are grateful to Dr Mark Hink for his help with the FCS and Dr P.M.P. van Bergen en Henegouwen for providing us with the cDNA of EGFR. We are very thankful to the people from the Laboratory of Virology, especially Magda Usmany for providing us with the assistance with insect cell cultures and Dr Just Vlak for some useful discussions. We especially thank Casper Vroemen for many useful discussions and critical comments on the manuscript. This work was supported by grants ERBIO4-CT96-2282 and ERBIO4-CT96-0689 from the EU Biotechnology program (K.S. and V.H.) and the Royal Netherlands Academy of Arts and Sciences (T.W.J.G.).

## References

1. Pawson, T. & Bernstein, A. (1990). Receptor tyrosine kinases: genetic evidence for their role in Drosophila and mouse development. *Trends Genet.* **6**, 350-356.
2. Cantley, L. C., Auger, K. R., Carpenter, C., Duckworth, B., Graziani, A., Kapeller, R. & Soltof, S. (1991). Oncogenes and signal transduction. *Cell,* **64**, 281-302.
3. Lease, K., Ingham, E. & Walker, J. C. (1998). Challenges in understanding RLK function. *Curr. Opin. Plant Biol.* **1**, 388-392.
4. Heldin, C. H. (1995). Dimerization of cell surface receptors in signal transduction. *Cell,* **80**, 213-223.
5. Bishayee, S., Majumdar, S., Khire, J. & Das, M. (1989). Ligand-induced dimerization of the platelet-derived growth factor receptor: monomer-dimer occurs independent of receptor phosphorylation. *J. Biol. Chem.* **264**, 11699-11705.
6. Westermark, B. & Heldin, C. H. (1989). Growth tactors and their receptors. *Curr. Opin. Cell Biol.* **25**, 1279-1285.
7. Lemmon, M. A. & Schlessinger, J. (1994). Regulation of signal transduction and signal diversity by receptor oligomerization. *Trends Biochem. Sci.* **19**, 459-463.
8. Schlessinger, J. (1988). Signal transduction by allosteric receptor oligomerization. *Trends Biochem. Sci.* **13**, 443-447.
9. Weiner, D. B., Kokai, Y., Wada, T., Cohen, J. A., Williams, W. V. & Greene, M. I. (1989). Linkage of tyrosine kinase activity with transforming ability of the p185neu oncoprotein. *Oncogene,* **4**, 1175-1183.
10. Spencer, D. M., Wandless, T. J., Schreiber, S. L. & Crabtree, G. R. (1993). Controlling signal transduction with synthetic ligands. *Science,* **262**, 1019-1024.
11. Jiang, G. & Hunter, T. (1999). Receptor signalling: when dimerization is not enough. *Curr. Biol.* **9**, 568-571.
12. Williams, R. W., Wilson, J. M. & Meyerowitz, E. M. (1997). A possible role of kinase-associated protein phosphatase in the *Arabidopsis* CLAVATA1 signaling pathway. *Proc. Natl Acad. Sci. USA,* **94**, 10467-10472.
13. Giranton, J. L., Dumas, C., Cock, J. M. & Gaude, T. (2000). The integral membrane S-locus receptor kinase of *Brassica* has serine/threonine kinase activity in a membranous environment and spontaneously forms oligomers in planta. *Proc. Natl Acad. Sci. USA,* **97**, 3759-3764.
14. Fletcher, J. C., Brand, U., Running, M. P., Simon, R. & Meyerowitz, E. M. (1999). Signaling of cell fate decisions by CLAVATA3 in Arabidopsis shoot meristems. *Science,* **283**, 1911-1914.
15. Jeong, S., Trotochaud, A. E. & Clark, S. E. (1999). The *Arabidopsis* CLAVATA2 gene encodes a receptor-like protein required for the stability of the CLAVATA1 receptor-like kinase. *Plant Cell,* **11**, 1925-1934.
16. Trotochaud, A. E., Jeong, S. & Clark, S. E. (2000). CLAVATA3, a multimeric ligand for the CLAVATA1 receptor-kinase. *Science,* **289**, 613-617.
17. He, Z., Wang, Z., Li, J., Zhu, Q., Lamb, C., Ronald, P. & Chory, J. (2000). Perception of brassinosteroids by the extracellular domain of the receptor kinase BRI1. *Science,* **288**, 2360-2363.
18. Nagayama, Y., Namba, H., Yokoyama, N., Yamashita, S. & Niwa, M. (1998). Role of asparagine-linked oligosaccharides in protein folding, membrane targeting, and thyrotropin and autoantibody binding of the human thyrotropin receptor. *J. Biol. Chem.* **273**, 33423-33428.
19. Trombetta, E. S. & Helenius, A. (1998). Lectins as chaperones in glycoprotein folding. *Curr Opin. Struct. Biol.* **8**, 587-592.
20. Elleman, T. C., Frenkel, M. J., Hoyne, P. A., McKern, N. M., Cosgrove, L. & Hewish, D. R. *et al.* (2000). Mutational analysis of the N-linked glycosylation sites of the human insulin receptor. *Biochem J.* **347**, 771-779.
21. Schmidt, E. D. L., Guzzo, F., Toonen, M. A. J. & de Vries, S. C. (1997). A leucine rich repeat containing receptor-like kinase marks somatic plant cells com-

petent to form embryos. *Development,* **124**, 2049-2062.
22. Gerdes, H. H. & Kaether, C. (1996). Green fluorescent protein: applications in cell biology. *FEBS Letters,* **389**, 44-47.
23. Ludin, B., Doll, T., Meili, R., Kaech, S. & Matus, A. (1996). Application of novel vectors for GFP-tagging of proteins to study microtubule-associated proteins. *Gene,* **173**, 107-111.
24. Carey, K. L., Richards, S. A., Lounsbury, K. M. & Macara, I. G. (1996). Evidence using a green fluorescent protein-glucocorticoid receptor chimera that the Ran/TC4 GTPase mediates an essential function independent of nuclear protein import. *J. Cell Biol.* **133**, 985-996.
25. Förster, T. (1948). Intermolecular energy migration and fluorescence. *Ann. Physik.* **6**, 55-75.
26. Johnson, I. D., Kang, H. C. & Haugland, R. P. (1991). Fluorescent membrane probes incorporating dipyrromethene boron difluoride fluorophores. *Anal. Biochem.* **198**, 228-237.
27. Rizzuto, R., Brini, M., De Giorgi, F., Rossi, R., Heim, R., Tsien, R. Y. & Pozzan, T. (1996). Double labelling of subcellular structures with organelle-targeted GFP mutants *in vivo*. *Curr. Biol.* **6**, 183-188.
28. Gadella, T. W. J., Jr, van der Krogt, G. & Bisseling, T. (1999). GFP-based FRET microscopy in living plant cells. *Trends Plant Sci.* **4**, 287-291.
29. Jovin, T. M. & Arndt-Jovin, D. J. (1989). Luminescence digital imaging microscopy. *Annu. Rev. Biophys. Chem.* **18**, 271-308.
30. Wu, P. & Brand, L. (1994). Resonance energy transfer: methods and applications. *Anal. Biochem.* **218**, 1-13.
31. Clegg, R. M. (1995). Fluorescence resonance energy transfer. *Curr. Opin. Biotechnol.* **6**, 103-110.
32. Chuck, R. S., Cantor, C. R. & Tse, D. B. (1990). CD4-T-cell antigen receptor complexes on human leukemia T cells. *Proc. Natl Acad. Sci. USA,* **87**, 5021-5025.
33. Vignali, D. A., Carson, R. T., Chang, B., Mittler, R. S. & Strominger, J. L. (1996). The two membrane proximal domains of CD4 interact with the T cell receptor. *J. Ex. Med.* **183**, 2097-2107.
34. Guo, C., Dower, S. K., Holowka, D. & Baird, B. (1995). Fluorescence resonance energy transfer reveals interleukin (IL)-1-dependent aggregation of IL-1 type I receptors that correlates with receptor activation. *J. Biol. Chem.* **270**, 27562-27568.
35. Carraway, K. L. & Cerione, R. A. (1993). Inhibition of epidermal growth factor receptor aggregation by an antibody directed against the epidermal growth factor receptor extracellular domain. *J. Biol. Chem.* **268**, 23860-23867.
36. Gadella, T. W., Jr & Jovin, T. M. (1995). Oligomerization of epidermal growth factor receptors on A431 cells studied by time-resolved fluorescence imaging microscopy. A stereochemical model for tyrosine kinase receptor activation. *J. Cell Biol.* **129**, 1543-1558.
37. Olson, T. S., Bamberger, M. T. & Lane, M. D. (1988). Post-translational changes in tertiary and quaternary structure of the insulin proreceptor. Correlation with acquisition of function. *J. Biol. Chem.* **263**, 7342-7351.
38. Bass, J., Chiu, G., Argon, Y. & Steiner, D. F. (1998). Folding of insulin receptor monomers is facilitated by the molecular chaperones calnexin and calreticulin and impaired by rapid dimerization. *J. Cell Biol.* **141**, 637-646.
39. High, S., Lecomte, F. J., Russell, S. J., Abell, B. M. & Oliver, J. D. (2000). Glycoprotein folding in the endoplasmic reticulum: a tale of three chaperones? *FEBS Letters,* **476**, 38-41.
40. Ullrich, A. & Schlessinger, J. (1990). Signal transduction by receptors with tyrosine kinase activity. *Cell,* **61**, 203-212.
41. Li, W. & Schlessinger, J. (1991). Platelet derived growth factor receptor (PDGFR)-induced dimerization of PDGF receptor in living cells. *Mol. Cell Biol.* **11**, 3756-3761.
42. Bai, M., Trivedi, S. & Brown, E. M. (1998). Dimerization of the extracellular calcium-sensing receptor (CaR) on the cell surface of CaR-transfected BEK293 cells. *J. Biol. Chem.* **273**, 23605-23610.
43. Fry, A. M., Arnaud, L. & Nigg, E. A. (1999). Activity of the human centrosomal kinase, Nek2, depends on an unusual leucine zipper dimerization motif. *J. Biol. Chem.* **274**, 16304-16310.
44. Baxevanis, A. D. & Vinson, C. R. (1993). Interactions of coiled coils in transcription factors: where is the specificity? *Curr. Opin. Genet. Dev.* **3**, 278-285.
45. Leung, W. & Lassam, N. (1998). Dimerization via tandem leucine zippers is essential for the activation of the mitogen-activated protein kinase kinase kinase, MLK-3. *J. Biol. Chem.* **273**, 32408-32415.
46. Kester, H. A., Blanchetot, C., den Hertog, J., van der Saag, P. T. & van der Burg, B. (1999). Transforming growth factor-beta-stimulated clone-22 is a member of a family of leucine zipper proteins that can homo and hetero dimerize and has transcriptional repressor activity. *J. Biol. Chem.* **274**, 27439-27447.
47. Behncken, S. N., Billestrup, N., Brown, R., Amstrup, J., Conway-Campbell, B. & Waters, M. J. (2000). Growth hormone (GH)-independent dimerization of GH receptor by a leucine zipper results in constitutive activation. *J. Biol. Chem.* **275**, 17000-17007.
48. Romano, C., Yang, W. L. & O'Malley, K. L. (1996). Metabotropic glutamate receptor 5 is a disulfide-linked dimer. *J. Biol. Chem.* **271**, 28612-28616.
49. Chen, R. H. & Derynck, R. (1994). Homomeric interactions between type II transforming growth factor-beta receptors. *J. Biol. Chem.* **269**, 22868-22874.
50. Henis, Y. I., Moustakas, A., Lin, H. Y. & Lodish, H. F. (1994). The types II and III transforming growth factor-beta receptors form homo-oligomers. *J. Cell Biol.* **126**, 139-154.
51. Cheatham, B. & Kahn, C. R. (1995). Insulin action and the insulin signaling network. *Endocrine Rev.* **16**, 117-142.
52. Trotochaud, A. E., Hao, T., Wu, G., Yang, Z. & Clark, S. E. (1999). The CLAVATA1 receptor-like kinase requires CLAVATA3 for its assembly into a signaling complex that includes KAPP and a Rho-related protein. *Plant Cell,* **11**, 393-406.
53. Schaller, G. E., Ladd, A. N., Lanahan, M. B., Spanbauer, J. M. & Bleecker, A. B. (1995). The ethylene response mediator ETR1 from Arabidopsis forms a disulfide-linked dimer. *J. Biol. Chem.* **270**, 12526-12530.
54. Doughty, J., Dixon, S., Hiscock, S. J., Willis, A. C., Parkin, I. A. & Dickinson, H. G. (1998). PCP-A1, a defensin-like Brassica pollen coat protein that binds the S locus glycoprotein, is the product of gametophytic gene expression. *Plant Cell,* **10**, 1333-1347.
55. Jiang, G., den Hertog, J., Su, J., Noel, J., Sap, J. & Hunter, T. (1999). Dimerization inhibits the activity of receptor-like protein-tyrosine phosphatase-alpha. *Nature,* **401**, 606-610.

56. Rezelman, G., van Kammen, A. & Wellink, J. (1989). Expression of cowpea mosaic virus mRNA in cowpea protoplasts. *J. Gen. Virol.* **70**, 3043-3050.
57. Rottier, P. J., Rezelman, G. & van Kammen, A. (1979). The inhibition of cowpea mosaic virus replication by actinomycin D. *Virology,* **92**, 299-309.
58. Groebe, D. R., Chung, A. E. & Ho, C. (1990). Cationic lipid-mediated co-transfection of insect cells. *Nucl. Acids Res.* **18**, 4033-4036.
59. Gadella, T. W., Jr, Vereb, G., Jr, Hadri, A. E., Rohrig, H., Schmidt, J. & John, M. *et al*. (1997). Microspectroscopic imaging of nodulation factor-binding sites on living *Vicia sativa* roots using a novel bioactive fluorescent nodulation factor. *Biophys. J.* **72**, 1986-1996.
60. Goedhart, J. & Gadella, T. W. J., Jr (2000). Advanced microspectroscopic methods for monitoring fluorescent molecules in living plant root hairs. In *Cell and Molecular Biology of Living Plant Root Hairs* (Ridge, R. W. & Emons, A. M. C., eds), pp. 65-93, Springer Verlag, Berlin.

***Edited by N.H. Chua***

*(Received 11 December 2000; received in revised form 16 April 2001; accepted 16 April 2001)*